Final Report to the Earthquake Commission on Project No. 10/CE618

Collection of seismic data from aftershocks of the 4 September 2010 M7.1 Darfield Earthquake

Principal Investigator

Martha K. Savage, Victoria University of Wellington (VUW)

Associate Investigators

Euan Smith, Tim Stern, John Townend (VUW),
Clifford Thurber, Ellen Syracuse (University of Wisconsin, Madison)

Contributing students

Robert Holt, MSc student
Kirsty Alan, Undergraduate summer scholar
Katrina Jacobs, PhDd student
Sapthalla Karaliyada, PhD student
Kathi Unglert, MSc student
Zara Rawlinson, MSc student
Jessica Johnson, PhD student
Pia Skorstengaard Undergraduate student
Aaron Johnston, Undergraduate summer scholar
Carolin Boese, PhD student

Technical assistance

Mark Henderson (VUW)

Layman's Abstract

We deployed 14 seismometers within 50 km of the Greendale Fault following the Sept. 4 2010 magnitude 7.1 Darfield earthquake. These operated until mid-January 2011. The data have been archived at the Incorporated Research Institutions for Seismology (IRIS) data center and at GNS Science. We used the data recorded by these instruments, supplemented by GeoNet broadband and strong-motion instruments, to study the changes in earthquake locations during the first four months of the aftershock sequence and the seismic anisotropy structure surrounding the fault. Earthquake relocations illuminate fault segments and show that the majority of aftershocks occurred beyond the areas of highest slip during the Darfield earthquake. Some of the earthquakes occurred on the fault that later broke in the February Christchurch earthquake. The lack of observable growth of seismicity along fault segments, suggests the Greendale Fault broke a pre-existing fault plane.

Contents:

Layman'sAbstract **(2)**

Technical Abstract **(3)**

Fulfilment of Objectives **(3)**

Publications resulting from this project **(5)**

Syracuse et al. NZJGG paper **(6)**

Technical Abstract

Following the Sept. 4 2010 Mw7.1 Darfield earthquake, with support from the Earthquake Commission and from the United States National Science Foundation, we deployed 4 broadband and 10 intermediate-period seismometers within 50 km of the Greendale Fault. These were operational until mid-January 2011. The data have been archived at the Incorporated Research Institutions for Seismology (IRIS) data center and at GNS Science. We used the data recorded by these instruments, supplemented by GeoNet broadband and strong-motion instruments, to study the spatio-temporal evolution of the first four months of the aftershock sequence and the seismic anisotropy structure surrounding the fault. Earthquake relocations illuminate fault segments and show that the majority of aftershocks occurred beyond the areas of highest slip during the Darfield earthquake. Some of the earthquakes occurred on the fault that later broke in the February Christchurch earthquake. Seismic anisotropy shows a mixture of fast directions parallel to the maximum horizontal stress and fault-parallel fast directions. This, combined with the lack of observable growth of seismicity along fault segments, suggests the Greendale Fault broke a pre-existing fault plane.

Fulfilment of Objectives

The main purpose of this proposal was to collect data for further analysis of the aftershocks of the Darfield earthquake. Here is our statement from the proposal:

We request funds to deploy the seismometers, including accommodation, air and ferry transport for people and equipment, and shipping for the US seismometers. We will plan to keep the seismometers out until January and have two site visits to change batteries and download data between now and then.

We have completed that main objective. We worked with Bill Fry at GNS science to determine the best locations of our instruments, taking into account the GNS short period locations. MSc student Zara Rawlinson also helped by running an early version of a code she was developing for her thesis, which involves determining the best locations for new seismic stations given a prior distribution of stations and seismicity. After the initial deployment, we made two more visits to change batteries, pick up data and check the instruments, in October and December, before pulling the instruments out in January. Figure 1 shows the station distributions, and Figure 2 shows the numbers of earthquakes located by GeoNet during the operation of the stations. The continuous data are now archived at the IRIS Data Management Center, at VUW, and at GNS Science.

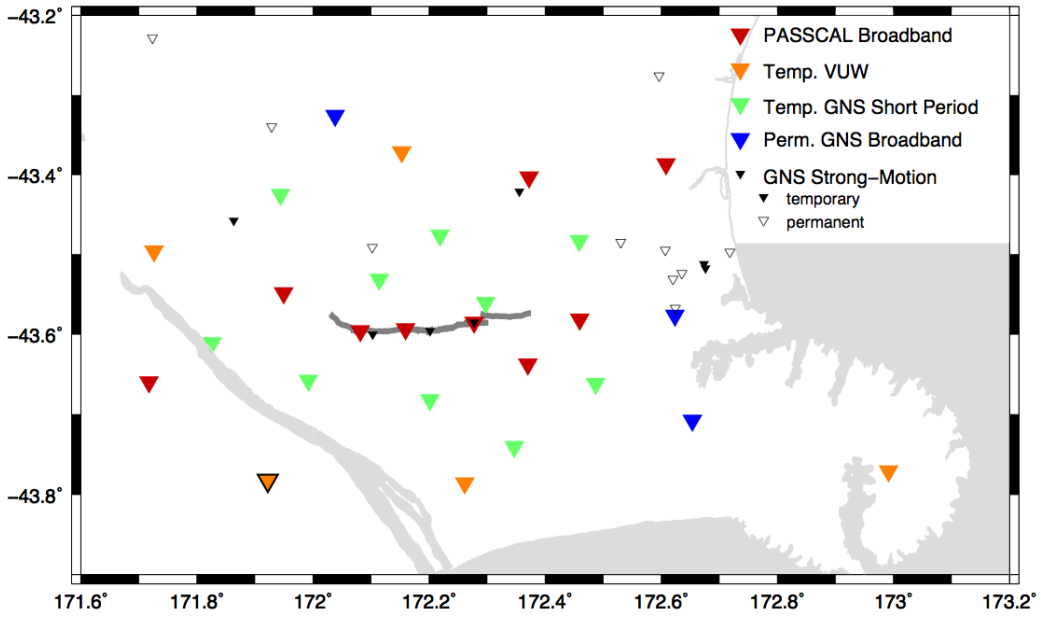

Figure 1. Map of temporary and permanent stations recording aftershocks of the Darfield earthquake that are being used in seismic tomography and other studies. VUW stations are broadband, except for the one in the southwest corner outlined in black, which is a 2 Hz seismometer. The strong-motion instruments shown are only those with GPS-clocks and no noted timing problems.

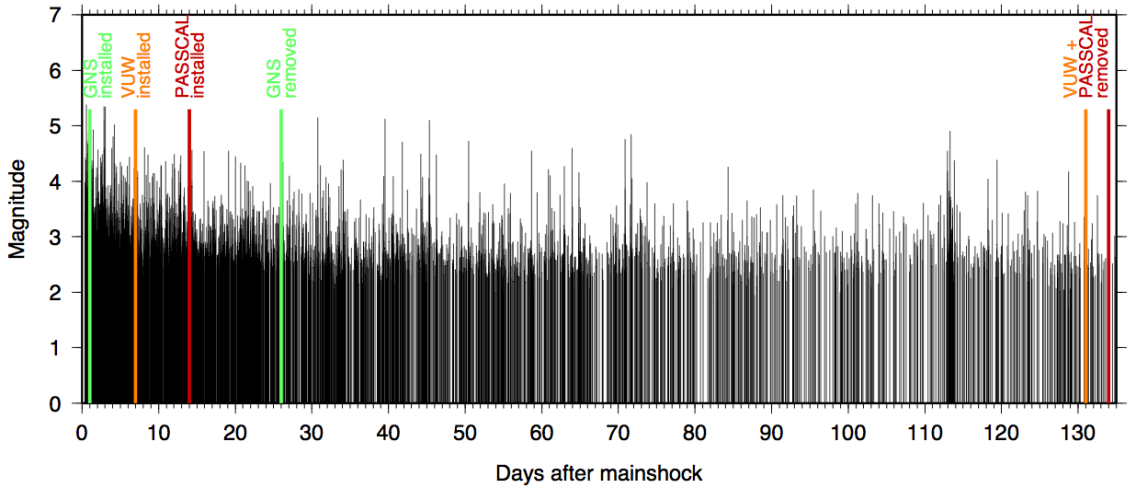

Figure 2. Plot of aftershocks for the first 90 days following the mainshock, scaled by magnitude. PASSCAL instruments were deployed from 15 to 17 days after the mainshock. Data source: http://magma.geonet.org.nz/resources/quakesearch/.

Because we required fewer funds than anticipated for our deployment, we were able to accomplish the additional goal of getting some of the seismograms' arrival times determined. We employed Kirsty Herbert and Aaron Johnston as summer research assistants to help to organise the data and also to help pick the arrival times. We also employed fourth-year students Rob Holt and Pia Skorstengaard to pick additional phases. Rob Holt completed a Diploma in Geophysics and is currently carrying out research for his MSc thesis, for which he has carried out shear wave splitting analysis. This preliminary analysis was used in the attached paper that is in press in the *New Zealand Journal of Geology and Geophysics*, and is also being used in subsequently funded research projects currently underway, also funded by EQC and NSF. The attached paper is one of the main outputs of this project, although it was completed with funding from the subsequent grants.

We also presented seven posters and talks at conferences such as the New Zealand Geoscience conferences in 2010 and 2011, the American Geophyiscal Union and the IRIS meeting in the USA.

Publications and presentations related to this project

Refereed publications

Syracuse EM, Holt RA, Savage MK, Johnson JH, Thurber CH, Unglert K, Allan KN, Karaliyadda S, Henderson M, Hypocentres and anisotropy from the Darfield aftershock sequence: Implications for fault geometry, age, and seismic property evolution, New Zealand Journal of Geology and Geophysics, accepted April 2012 (this volume was co-edited by AI John Townend).

Postgraduate Diploma of Science in Geophysics thesis

Robert A. Holt: Shear wave splitting on the Canterbury Plains: The nature of the Greendale Fault, 33 pp.

Conference abstracts presented related to this project:

Rob A. Holt, Jessica H. Johnson, Ellen M. Syracuse, Martha K. Savage, Clifford H. Thurber, Mark Henderson, Kirsty Allan, Katharina Unglert, Shear wave splitting and evolution of seismicity on the Canterbury plains: The nature of the Darfield fault, Poster given at *Eos Trans. AGU, 92(52)*, Fall Meet. Suppl., Abstract S31C-2254, 2011.

R.A. Holt, M.K. Savage, E.M. Syracuse, C.H. Thurber, M. Henderson, K. Allan, and K. Unglert, Shear wave splitting on the Canterbury plains: The nature of the Darfield fault In: Litchfield, N.J., Clark, K. (eds). Abstract volume, Geosciences 2011 Conference, Nelson, New Zealand. Geoscience Society of New Zealand Miscellaneous Publication 130A: p. 50, 2011

M. Savage, C. Boese, Y. Behr, K. Jacobs, S. Karalliyadda, K. Unglert et. al., Search for time-varying seismic properties after the 2010 M7.1 Darfield earthquake, poster given at the GeoNZ 2010 Conference, Incorporating the Geoscience Society of New Zealand Conference and the New Zealand Geothermal Workshop, 21-24th November 2010, The University of Auckland.

M.K. Savage, E.M. Syracuse, J. Johnson, R. Holt, K. Unglert, C.H. Thurber, M. Henderson, N. Lord, and K. Allan, Temporal evolution of the Darfield aftershock sequence prior to the Christchurch earthquake, In: Litchfield, N.J., Clark, K. (eds). Abstract volume, Geosciences 2011 Conference, Nelson, New Zealand. Geoscience Society of New Zealand Miscellaneous Publication 130A: p. 57, 2011.

M. Henderson, C. Boese, M. Savage, B. Fry, C. Thurber, K. Jacobs et. al. Aftershocks of the 4 Septemer 2010 M7.1 Darfield Earthquake, poster given at the GeoNZ 2010 Conference, Incorporating the Geoscience Society of New Zealand Conference and the New Zealand Geothermal Workshop, 21-24th November 2010, The University of Auckland.

A. Zaino, P. Malin, A. Doran, M. Savage, C. Thurber, E. Syracuse, N. Lord, and M. Henderson, Fault guided waves in the Darfield aftershock sequence, in: Litchfield, N.J., Clark, K. (eds). Abstract volume, Geosciences 2011 Conference, Nelson, New Zealand. Geoscience Society of New Zealand Miscellaneous Publication 130A: p. 121, 2011.

E.M. Syracuse, R.A. Holt, M.K. Savage, J.H. Johnson, C.H. Thurber, K. Unglert, K.N. Allan, S. Karaliyadda, M. Henderson, Hypocentres and anisotropy from the Darfield aftershock sequence: Implications for fault geometry, age, and seismic property evolution, 2012 IRIS Workshop, Boise, Idaho.

Temporal and spatial evolution of hypocentres and anisotropy from the Darfield aftershock sequence: Implications for fault geometry and age

Ellen M. Syracuse[1], Rob A. Holt[2], Martha K. Savage[2], Jessica H. Johnson[2,3], Clifford H. Thurber[1], Katharina Unglert[2,4], Kirsty N. Allan[2], Sapthalla Karaliyadda[2], Mark Henderson[2,5]

1. Department of Geoscience, University of Wisconsin-Madison
2. Institute of Geophysics, Victoria University of Wellington, New Zealand
3. Now at: University of Hawaii at Hilo/Hawaii Volcano Observatory, US Geological Survey
4. Now at: Department of Earth and Ocean Sciences, The University of British Columbia, Vancouver, Canada
5. Now at: GNS Science, New Zealand

Abstract

The first four months of aftershocks of the Darfield earthquake have been studied using data from temporary and permanent seismic stations to investigate the fault geometry, stress field, and evolution of seismicity and seismic properties. Earthquake relocations illuminate fault segments and show that the majority of aftershocks occurred beyond the areas of highest slip during the Darfield earthquake. Seismic anisotropy shows a mixture of fast directions parallel to the maximum horizontal stress σ and fault-parallel fast directions. This, combined with the lack of observable growth of seismicity along fault segments, suggests the Greendale Fault broke a pre-existing fault plane.

Introduction

Following the M_w7.1 Darfield earthquake (discussed in this volume) we deployed 4 broadband and 10 intermediate-period seismometers within 50 km of the Greendale Fault, which were operational until mid-January 2011 (Figure 1). The data recorded by these instruments, supplemented by GeoNet broadband and strong-motion instruments, have been analysed to study the evolution of the first four months of the aftershock sequence and the seismic anisotropy structure surrounding the fault.

Hypocentral Relocations

Hypocentres have been calculated for 2827 aftershocks (Figure 1) using the double-difference algorithm tomoDD (Zhang & Thurber 2003), which uses absolute arrival, differential catalogue, and cross-correlated differential times. P- and S-arrivals for temporary stations were hand-picked. Initial locations are from the GeoNet catalogue and the 1D velocity model used for relocation is based on average velocities in the Canterbury region from the Eberhart-Phillips et al. (2010) model.

Catalogue differential times were calculated from the absolute times for pairs of neighbouring earthquakes recorded by at least 6 common stations. Cross-correlated differential times were calculated using the bispectrum

verification method of Du et al. (2004), which decreases the sensitivity of the correlation to noise and increases the precision of the differential times. The three data types were weighted progressively throughout the inversion, with absolute arrival times weighted most heavily in earlier iterations to establish absolute locations, and differential times weighted more heavily in later iterations to refine the seismicity distribution. Average absolute arrival time residuals were reduced from 387 ms for P-arrivals and 725 ms for S-arrivals to 145 ms and 324 ms, respectively.

Recent analysis of geodetic and seismic waveform data has identified six fault segments active during the Darfield earthquake (Figure 1; Beavan et al. 2011): three of these segments (A-C) form the Greendale Fault and the remaining three are the blind Charing Cross reverse fault (segment D), on which the mainshock rupture is believed to have begun, a blind reverse fault west of the surface rupture (segment E), and a SW-NE fault near the left-step of the surface rupture (segment F). The relocations presented here help refine the orientations and extents of these fault segments.

The relocated seismicity forms a band as narrow as 3-km (measured N-S) beneath the central part of the surface rupture, less than half as wide as from catalogue locations, with an average depth of 8.7 km (Figure 1). Given the density of intersecting fault segments beneath the surface rupture and uncertainty about which fault individual aftershocks occurred on, it is difficult to verify the dips of the Greendale Fault segments proposed by Beavan et al. (2010). However, it is clear that the fault beneath the centre of the surface rupture is subvertical (segments A and C) and segment B beneath the western portion of the surface rupture dips to the northeast, as in the Beavan model.

The only fault segment where relocated seismicity clearly differs in dip from the Beavan model is segment E, the NW-dipping blind reverse fault west of the surface rupture. However, our proposed dip is a modest change from that model: 50-55° versus 65° in Beavan's model. This segment also contains earthquakes with the largest epicentral differences between our relocations and the catalogue locations. The 4-km NW shift in our relocations is attributed to the greater distance from nearby GeoNet stations (>29 km) in comparison to aftershocks further east, whereas these relocations are improved by the close proximity (<5 km on average) to the nearest temporary station. Based on several relocated earthquakes near the Rakaia River, it is possible that this fault segment extends 10 km or more west of the initial estimate.

In comparison to the geodesy- and waveform-derived slip distributions in the Beavan model, the relocated seismicity occurs at least 5 km below the regions of highest slip for each fault segment, with the exception of segment F near the surface rupture stepover (Figure 2). In this SW-NE fault segment, aftershock seismicity is co-located with the area of highest seismic slip. With the exception of this segment, the seismically active area of each fault segment is larger than the area activated in the initial rupture of the Darfield earthquake.

Seismic Anisotropy

We used the MFAST (Savage et al. 2010) automatic shear wave splitting

technique to determine the fast axis of the anisotropic medium (ϕ) and the delay time between the rotated horizontal components (dt). The MFAST method uses the technique of Silver and Chan (1991) on a window surrounding the S-arrival to determine the best-fitting ϕ and dt as measured by the most linear particle motion of waveforms after correcting for assumed splitting. The frequency content of the waveform is used to determine the start and end times for multiple windows and cluster analysis is used to determine the best measurement over the windows (Teanby et al. 2004). An automatic grading system is carried out; we present the highest-quality results. The S-arrival times are the same as used for the earthquake relocations. Most of the S-phases arrive with near-vertical incidence angles.

Most ϕ (Figure 3), particularly for stations in the centre and northwest of the array, are nearly parallel to the maximum horizontal stress direction (σ_{Hmax}) as expected for vertically aligned cracks (e.g., Nur 1969). Strong alignment of ϕ at most stations, despite wide variation in propagation azimuth (Figure 4), suggests that radial anisotropy is not affecting the results. However, there is inter-station variability, with MQZ having nearly perpendicular orientations and Bnk1 having a population parallel to σ_{Hmax} and one parallel to a lineation inferred by Sibson et al. (2011) to be a conjugate left-lateral strike-slip fault. Stations Cch1 and Cch4 have one population parallel to σ_{Hmax} and one parallel to the Greendale fault rupture. Station Dar6, located near the stepover in the surface rupture, has nearly fault-parallel ϕ. Stations Dar4 and Dar8 are on fault segment B, which strikes sub-parallel to the maximum principal stress, so ϕ for these stations is both fault-parallel and parallel to σ_{Hmax}. Several of the other stations have fast directions that are nearly fault-parallel for earthquakes that occur near the fault plane (Figure 4). Apparent temporal changes in ϕ or dt at some stations are attributed to changes in earthquake distribution (Figure 4).

Multiplets

We used the method of Du et al. (2004) to identify multiplets. A window of 2.54 seconds around the P-arrival was used with a Hanning tapered band-pass filter between 1 and 10 Hz. Multiplets were identified by having a P-wave cross-correlation coefficient of more than 0.90 at two or more stations. One of the longest-lived multiplets includes events from September through 10 February, twelve days before the Christchurch earthquake. Figure 5 shows the waveforms for this multiplet at station MQZ. The S-waveforms here are not as well correlated as the P-waveforms, as confirmed by an overlay of each phase and the small amplitude of the S-arrival stack.

Discussion

Stress field and fault reactivation

The anisotropy must occur in the upper crust, between the earthquakes and stations. Generally, ϕ is parallel to σ_{Hmax} (Leitner et al. 2001; Balfour et al. 2005; Sibson et al. 2011), suggesting that stress-aligned microcracks cause the anisotropy. However, fault-parallel ϕ is also observed at Dar6, directly over the

fault, and at Dar4 and Dar8, which are on fault segments parallel to the regional stress. Moreover, other stations also show fault-parallel ϕ for events near the fault and yield other directions for off-fault earthquakes (e.g., Dar 1; Dar6 in Figure 4). Similar behaviour was found in California, where earthquakes near the Calaveras Fault yielded fault-parallel anisotropy and those away from it were more parallel to the regional σ_{Hmax} (Zinke & Zoback 2000). Fault fabric may be aligned strongly enough over the S-wavelengths (220 m for the near-surface S-wave) to produce anisotropy. Vertical aligned cracks and vertical faults both require a "wrench-type" fault regime in which σ_2 is vertical and σ_3 and σ_1 are horizontal (Anderson, 1951). Sibson et al. (2011) suggests that the 30° difference between the Greendale Fault and the prevailing stress field means that it is either a fairly newly formed fault or a reactivated one that happens to be optimally oriented. The anisotropy suggests that the fault fabric has developed over a relatively long period and that it is a reactivated fault. Parallelism between seismic anisotropy and major strike-slip fault orientations has also been found just north of here in the Marlborough region (Balfour et al. 2005).

If the Greendale Fault system were young, one may expect to observe an increase in fault area over time. While aftershock seismicity extends beyond the modelled rupture planes of the Darfield earthquake (Beavan et al. 2010), there is no clear expansion of fault planes through the four months of aftershocks analysed here (Figure 2). In fact, the reverse occurs; earthquakes within two weeks of the mainshock are 2 km deeper, on average, than those over the following four months. If there was any identifiable temporal growth of faults, it occurred within the first two weeks of the aftershock sequence.

Fault orientations

In addition to the seismically active fault segments identified in Beavan et al. (2010) and in this study, a seventh segment is characterised by a NNW-SSE band of seismicity extending from the centre of the surface rupture to 18 km north of it (segment G in Figure 1), which is also required by ALOS data (Elliot et al. 2012) The seismicity within this plane has an orientation of 350° and is 4 km wide E-W. Based on the seismicity, the plane dips to the west at an angle likely steeper than 65°, with aftershocks from the surface to 16.1 km depth. However, the fault in the Elliot et al. (2012) model dips steeply to the east. Preliminary focal mechanisms calculated for earthquakes along this segment using HASH (Hardebeck & Shearer 2002) indicate left-lateral motion. This is consistent with newly formed ductile shears in the current stress regime (Sibson et al. 2011).

Immediately west of where segment G nears the centre of the Greendale Fault surface rupture is the blind Charing Cross reverse fault, where the Darfield earthquake initiated (Beavan et al. 2010). Interestingly, the Charing Cross Fault appears to have few aftershocks on it; most relocated seismicity in this area is either beneath the Greendale Fault surface rupture or within segment G.

Time dependence of seismicity and seismic properties

While aftershocks within a month of the Darfield earthquake were relatively evenly distributed along the fault trace and ~25 km beyond its ends,

seismicity beneath the surface rupture decreased in frequency while aftershocks on secondary faults persisted at higher rates. By late November, there was less than one aftershock per day west of the surface rupture, whereas seismicity in the dilatational stepover and to its east continued at a relatively higher rate, as exemplified by the M4.9 Boxing Day earthquake and its own aftershocks (Figure 2). Beneath Christchurch, aftershocks occurred in sporadic clusters throughout the study period. This seismicity was shallower than almost all aftershocks nearer to the Greendale Fault, at an average of 5.3 km depth, consistent with depths of relocated aftershocks of the 22 February Christchurch earthquake (Bannister et al. 2011). A weak lineation in the post-Darfield but pre-Christchurch aftershocks occurred sub-parallel and slightly north of the fault directly responsible for the Christchurch earthquake and extended southwest to the dilatational stepover (segment H, Figure 1), indicating that fault may extend further southwest than indicated by other models (e.g., Kaiser et al. 2012) and may have been stressed throughout the 5.5-month-long period leading to the Christchurch earthquake.

The apparent temporal changes in seismic anisotropy observed at some stations, such as MQZ, can be explained by spatial variations in anisotropy combined with migration of epicentres (Figure 4), so that changes in stress or seismic properties with time are not required. At MQZ, earthquakes in the Christchurch area yield smaller dt and more E-W ϕ than those in other areas.

Although P-waveforms for the multiplet shown were highly correlated, the S-waveforms were not. At MQZ, the S energy for this multiplet arrived earlier in January and February 2011 than in September 2010 (Figure 5), confirmed by horizontal component data (not shown). There was no migration of relocated hypocentres over time, so raypath length changes do not explain the early arrivals. Healing cracks along the raypath of the multiplets would be consistent with an earlier S-arrival; however, the average Vp/Vs ratio at that station did not decrease over time, and the S-waveforms change character rather than “stretching” as is seen in some studies showing crack healing (e.g., Li et al. 1998). The S-waveform evolution may be caused by structural changes along the path during the earthquake sequence, resulting in scattered energy arriving at different times (e.g., Niu et al. 2003).

Conclusions

- Earthquake hypocenters occurred mostly outside and below the region of maximum slip of the Darfield earthquake.
- A newly identified lineation of seismicity (segment G) is consistent with ALOS geodetic inversions (Elliot et al. 2012) and with the direction expected for newly formed ductile shears (Sibson et al. 2011), and another lineation delineates the eventual fault plane of the Feb. 22 earthquake.
- Some of the local anisotropy may be caused by stress-induced microcracks, while structurally controlled, fault-parallel anisotropy is observed close to the mainshock fault plane.

- Fault-parallel anisotropy plus the lack of fault-plane growth over time suggests the main Darfield earthquake broke a pre-existing fault plane.
- Multiplets with highly correlated P-waves show changes in S-waveforms over time, suggesting evolving scatters along the raypath.

Acknowledgements

This work was funded by grants from the New Zealand Earthquake Commission, the National Science Foundation, and GNS Science. GNS Science Wairakei, University of Auckland and PASSCAL RAMP provided instrumentation. Field assistants included A. Zaino, J. Eccles, K. Jacobs, C. Boese, R. Davy, A. Wech, N. Lord, and A. Carrizales. Z. Rawlinson, J. Townend, P. Malin, and B. Fry helped plan station locations. Arrivals were determined by GeoNet processors for permanent stations and by the authors, P. Skorstengaard, R. Hart, and G. Potaka for temporary stations. We also thank the editor and reviewers for their helpful comments.

References

Anderson, E.M. (1951). *The Dynamics of Faulting and Dyke Formation with Application to Britain (2nd edn.)*. Oliver & Boyd, Edinburgh, 206 pp.

Balfour, N. J., Savage, M. K., Townend, J. 2005. Stress and crustal anisotropy in Marlborough, New Zealand: Evidence for low fault strength and structure-controlled anisotropy, Geophysical Journal International, 163 (3), 1073-1086, doi: 10.1111/j.1365-246X.2005.02783.x.

Bannister, S., Fry, B., Reyners, M., Ristau, J. and Zhang, H. 2011. Fine-scale relocation of aftershocks of the 22 February M_w 6.2 Christchurch earthquake using double-difference tomography, Seismological Research Letters, 82(6): 839-845.

Beavan, J., Samsonov, S., Motagh, M., Wallace, L. and Ellis, S. 2010. The Darfield (Canterbury) earthquake: Geodetic observations and preliminary source model, Bulletin of the New Zealand Society for Earthquake Enginerering, 43(4): 228-235.

Du, W.-X., Thurber, C. H. and Eberhart-Phillips, D. 2004. Earthquake relocation using cross-correlation time delay estimates verified with the bispectrum method, Bulletin of the Seismological Society of America, 94(3): 856-866.

Eberhart-Phillips, D., Reyners, M., Bannister, S., Chadwick, M. and Ellis, S.2010. Establishing a Versatile 3-D Seismic Velocity Model for New Zealand, Seismological Research Letters, 81(6): 992-1000, doi:10.1785/gssrl.81.6.992.

Elliot, J. R., Nissen, E. K., England, P. C., Jackson, J. A., Lamb, S. Li, Z., Oehlers, M. and Parsons, B. 2012. Slip in the 2010-2011 Canterbury earthquakes, New Zealand, Journal of Geophysical Research, 117, B03401, doi:10.1029/2011JB008868.

Hardebeck, J. L. and Shearer, P. M. 2002. A new method for determining first-motion focal mechanisms, Bulletin of the Seismological Society of America, 92, 2264-2276.

Leitner, B., Eberhart-Phillips, D., Anderson, H., and Nabelek, J. 2001. A focused

look at the Alpine Fault, New Zealand: seismicity, focal mechanisms and stress observations. Journal of Geophysical Research, 106, 2193-2220, doi:10.1029/2000JB900303.

Li, Y. G., Burdette, T., Vidale, J. E., Aki, K. and Xu, F. 1998. Evidence of shallow fault zone strengthening after the 1992 M7.5 Landers, California, earthquake, Science, 279(5348), 217-219.

Kaiser, A., Holden, C., Beavan, J., Beetham, D., Benites, R., Celentano, A., Collet, D., Cousins, J., Cubrinovski, M., Dellow, G., Denys, P., Fielding, E., Fry, B., Gerstenberger, M., Langridge, R., Masset, C., Motagh, M., Pondard, N., McVerry, G., Ristau, J., Stirling, M., Thomas, J., Uma, S.R., and Zhao, J. 2012. The M_W 6.2 Christchurch earthquake of February 2011: preliminary report, New Zealand Journal of Geology and Geophysics, 55, 1-24, doi:10.1080/00288306.2011.641182

Niu, F. L., Silver, P. G., Nadeau, R. M. and McEvilly, T. V. 2003. Migration of seismic scatters associated with the 1993 Parkfield aseismic transient event, Nature, 426, 544-548, doi:10.1038/nature02151.

Nur, A. and Simmons, G. 1969. The effect of saturation on velocity in low porosity rocks, Earth and Planetary Science Letters, 7(2), 183-193, doi:10.1016/0012-821X(69)90035-1.

Quigley, M., Villamor, O., Furlong, K., Beavan, J., Van Dissen, R., Litchfield, N., Stahl, T., Duffy, B., Bilderback, E., Noble, D., Barrel, D., Jongens, R. and Cox, S. 2010, Previously unknown fault shakes New Zealand's South Island, EOS, Transactions, American Geophysical Union, 91 (49), 469-471.

Savage, M. K., Wessel, A., Teanby, N. A. and Hurst, A. W. 2010. Automatic measurement of shear wave splitting and applications to time varying anisotropy at Mount Ruapehu volcano, New Zealand, Journal of Geophysical Research, 115, B12321, doi:10.1029/2010JB007722.

Sibson, R., Ghisetti, F. and Ristau, J. 2011. Stress control of an evolving strike-slip fault system during the 2010-2011 Canterbury, New Zealand, earthquake sequence, Seismological Research Letters, 82(6):824-832.

Silver, P. G. and Chan, W. W. 1991. Shear wave splitting and subcontinental mantle deformation, Journal of Geophysical Research, 96: 16429-16454.

Teanby, N., Kendall, J.-M. and can der Baan, M. 2004. Automation of shear-wave splitting measurements using cluster analysis, Bulletin of the Seismological Society of America, 94:453-463.

Zhang, H. and Thurber, C. H. 2003. Double-difference tomography: The method and its application to the Hayward Fault, California, Bulletin of the Seismological Society of America, 93(5): 1875-1889.

Zinke, J. C. and Zoback, M. D. 2000.Structure-related and stress-induced shear-wave velocity anisotropy: observations from microearthquakes near the Calaveras Fault in central California. Bulletin of the Seismological Society of America. 90, 1305-1312.

#

#

Figures

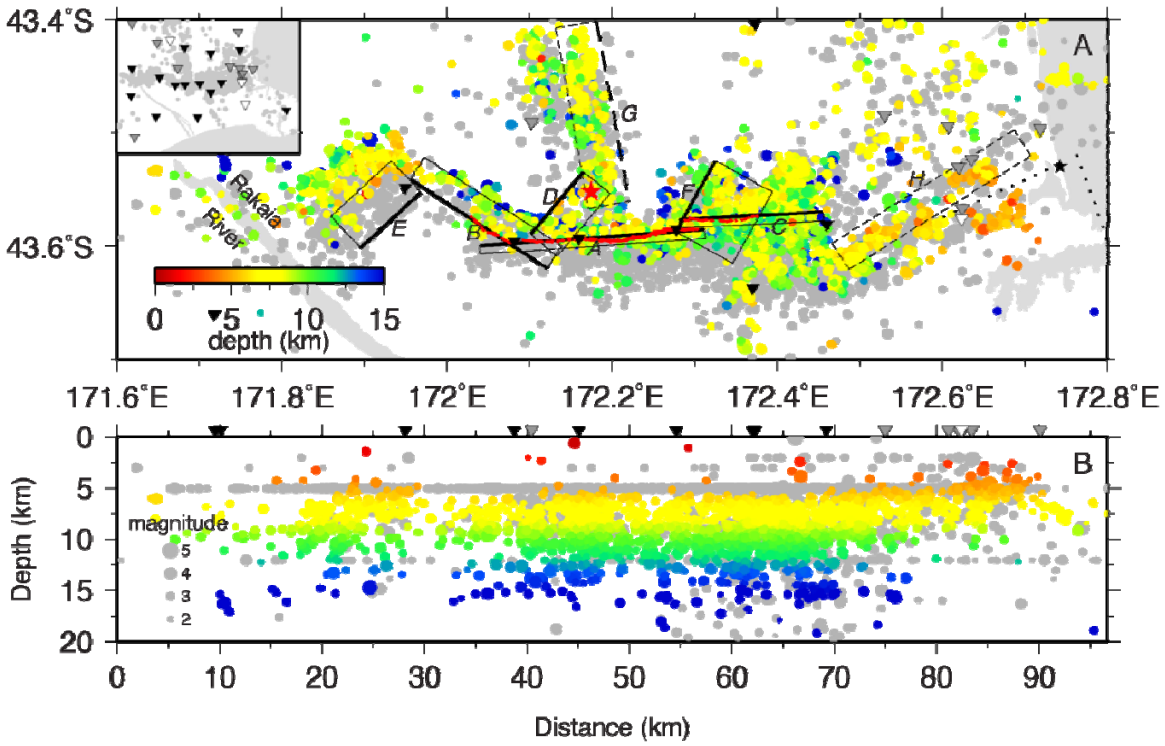

Figure 1: Relocated aftershock seismicity. A. Map showing relocated seismicity (coloured circles) and GeoNet catalogue seismicity (grey), scaled by magnitude. Inverted triangles show stations: temporary instruments (black), permanent GeoNet stations (white), and permanent strong-motion stations (grey). The red line indicates the surface rupture of the Darfield earthquake (Quigley et al., 2010) and the red star indicates its epicentre. Labelled bold black lines indicate the updip extents of fault planes from Beavan et al. (2010), with thinner solid lines representing their downdip extents. Dashed lines indicate fault segments G and H, identified in this study. Dotted lines indicate faults beneath Christchurch (Beavan et al., 2011), which ruptured after the earthquakes presented here. The black star indicates the epicentre of the February 2011 Christchurch earthquake. Inset map shows all stations used in this study. B, W-E cross-section showing earthquakes from panel A.

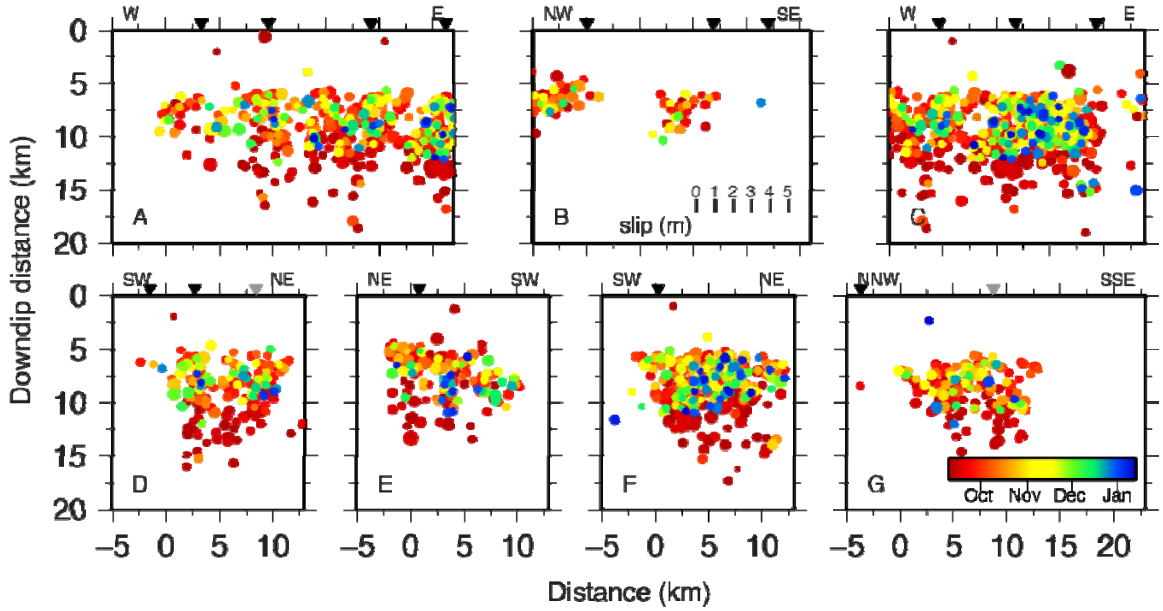

Figure 2: Cross sections of relocated seismicity within 5 km of the faults described in Beavan et al. (2010), overlain on the slip model from that study, and fault segment G, assuming a vertical fault. Grey vectors indicate the modelled slip of the hanging wall relative to the footwall.

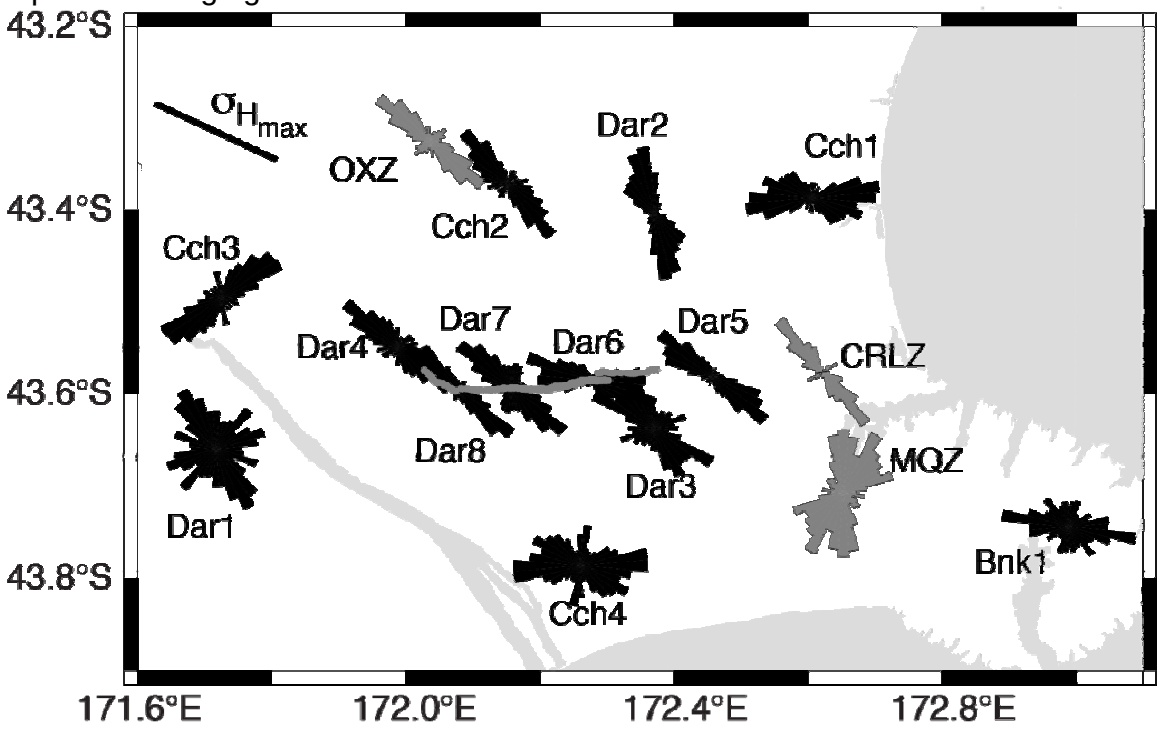

Figure 3: Rose diagrams showing ϕ for temporary stations (black) and permanent GeoNet stations (grey). The surface rupture is shown in grey and σ_{Hmax} is oriented at 115°, indicated by the black line (Leitner et al., 2001).

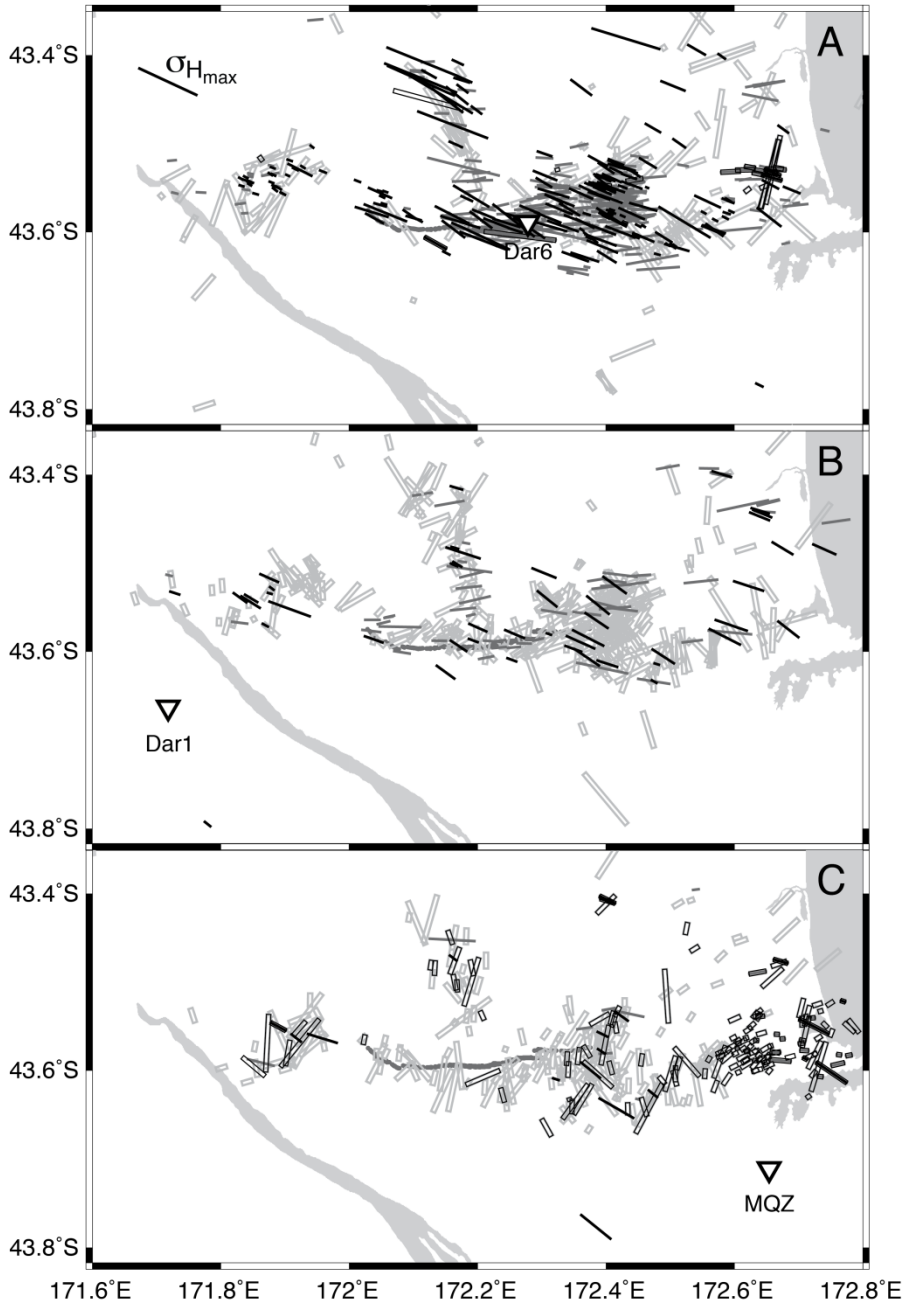

Figure 4: Individual measurements for A, Dar6, B, Dar1, and C, permanent station MQZ, plotted at the GeoNet earthquake locations. Station MQZ has more measurements because it includes all earthquakes between September 2010 and April 2011. Bars are parallel to ϕ and their length is proportional to dt. The maximum dt (0.4 s) is shown by the black bar in A, oriented parallel to the regional σ_{Hmax}. Solid grey bars indicate splitting sub-parallel to the fault, black indicates splitting sub-parallel to σ_{Hmax}, and grey outlines indicate all other ϕ. Black outlines show measurements following the Boxing Day earthquake and display no discernable temporal variation.

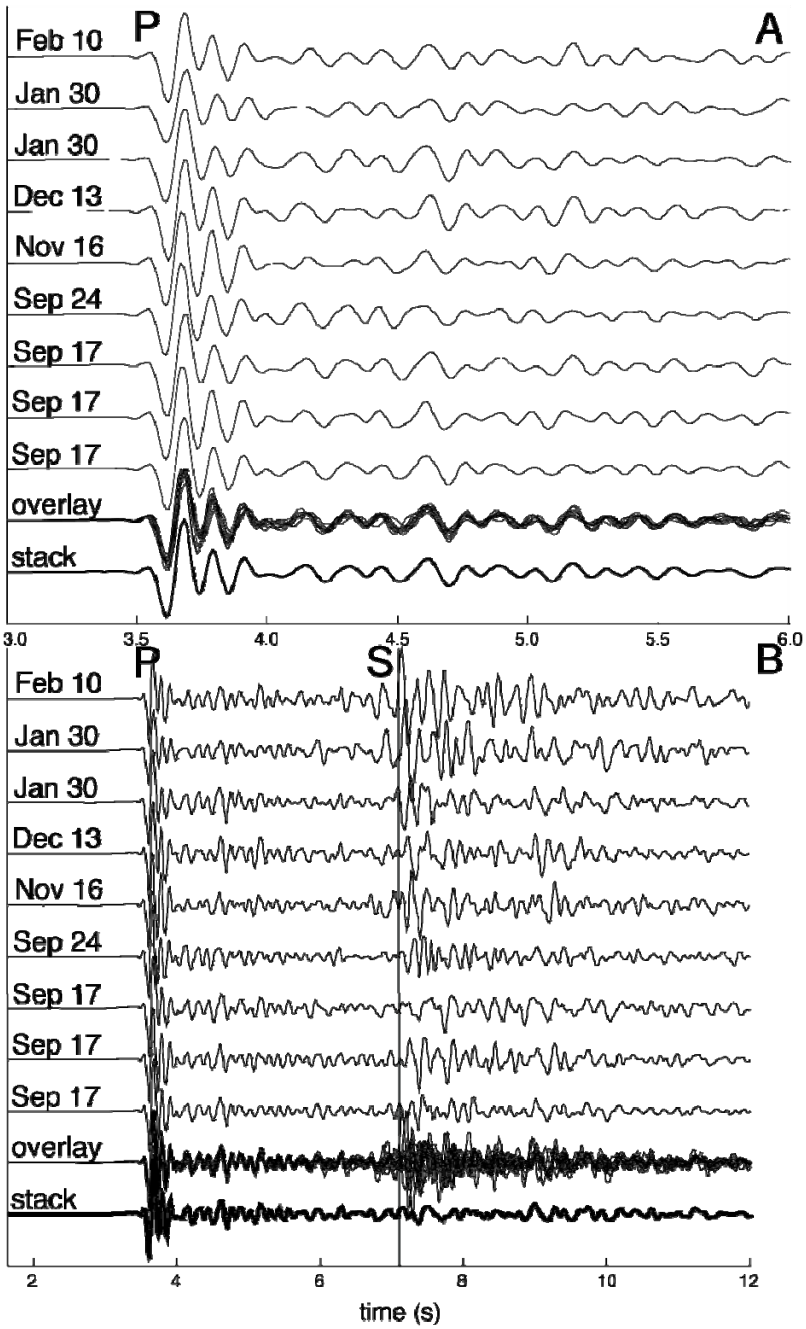

Figure 5: Vertical components from the 17 September - 10 February multiplet recorded at station MQZ. A, P-waveforms of nine events with correlation coefficients greater than 0.95, aligned on the time of the maximum cross correlation. B, S-waveforms for the same earthquakes. The vertical line is at the start of the S-wave train for the first two events.